REPORT DOCUMENTATION PAGE

Form Approved
OMB No. 0704-0188

1. REPORT DATE *(DD-MM-YYYY)*
13-04-2011

2. REPORT TYPE
Article

3. DATES COVERED *(From - To)*
MAR 2011 - APR 2011

4. TITLE AND SUBTITLE
Limits to Maximum Absorption Length in Waveguide Photodiodes

5a. CONTRACT NUMBER
FA8720-05-C-0002

5b. GRANT NUMBER

5c. PROGRAM ELEMENT NUMBER

6. AUTHOR(S)
Shannon M. Madison, Jonathan Klamkin, Douglas C. Oakley, Antonio Napoleone, Jason J. Plant, and Paul W. Juodawlkis

5d. PROJECT NUMBER

5e. TASK NUMBER

5f. WORK UNIT NUMBER

7. PERFORMING ORGANIZATION NAME(S) AND ADDRESS(ES)
MIT Lincoln Laboratory
244 Wood Street
Lexington, MA 02420

8. PERFORMING ORGANIZATION REPORT NUMBER

9. SPONSORING / MONITORING AGENCY NAME(S) AND ADDRESS(ES)
AFLCMC/PZE
20 Schilling Circle, Bldg 1305
Hanscom AFB, MA 01731

10. SPONSOR/MONITOR'S ACRONYM(S)
AFLCMC/PZE

11. SPONSOR/MONITOR'S REPORT NUMBER(S)

12. DISTRIBUTION / AVAILABILITY STATEMENT
DISTRIBUTION STATEMENT A. Approved for public release; distribution is unlimited.

13. SUPPLEMENTARY NOTES

14. ABSTRACT
The maximum photocurrent, power dissipation, and linearity of waveguide photodiodes are limited by the length over which the input optical power is absorbed. This absorption length is determined by the absorption coefficient of the absorbing layer material (a0), the optical confinement factor (r), and the excess optical loss (ai). In this work, we analyze the fundamental limits to maximizing the absorption length and demonstrate a new waveguide photodiode structure that approaches these limits. The new structure is referred to as a slab-coupled optical waveguide photodiode (SCOWPD) and is realized in the InGaAsP/InP material system. Assuming 100% coupling efficiency, the SCOWPD has an ultra-low optical confinement factor and low excess optical loss, both calculated from measurements, of r = 0.069% and ai = 1.65 cm^-1, respectively. This results in a 1/e absorption length of 2.1 mm. The SCOWPD exhibits an external responsivity of 0.8 A/W and a maximum photocurrent of 250 mA at a wavelength of 1.55 um.

15. SUBJECT TERMS
p-i-n photodiodes, optical waveguides, analog optical links, optical confinement factor, waveduide photodiode

16. SECURITY CLASSIFICATION OF: U			17. LIMITATION OF ABSTRACT	18. NUMBER OF PAGES	19a. NAME OF RESPONSIBLE PERSON Zach Sweet
a. REPORT U	**b. ABSTRACT** U	**c. THIS PAGE** U	SAR	11	**19b. TELEPHONE NUMBER** *(include area code)* 781-981-5997

JA-18524

Limits to Maximum Absorption Length in Waveguide Photodiodes

Shannon M. Madison, Jonathan Klamkin, *Member, IEEE*, Douglas C. Oakley, Antonio Napoleone, Jason J. Plant, and Paul W. Juodawlkis, *Senior Member, IEEE*

Abstract: The maximum photocurrent, power dissipation, and linearity of waveguide photodiodes are limited by the length over which the input optical power is absorbed. This absorption length is determined by the absorption coefficient of the absorbing layer material (α_o), the optical confinement factor (Γ), and the excess optical loss (α_i). In this work, we analyze the fundamental limits to maximizing the absorption length and demonstrate a new waveguide photodiode structure that approaches these limits. The new structure is referred to as a slab-coupled optical waveguide photodiode (SCOWPD) and is realized in the InGaAsP/InP material system. Assuming 100% coupling efficiency, the SCOWPD has an ultra-low optical confinement factor and low excess optical loss, both calculated from measurements, of $\Gamma = 0.069\%$ and $\alpha_i = 1.65$ cm^{-1}, respectively. This results in a 1/*e* absorption length of 2.1 mm. The SCOWPD exhibits an external responsivity of 0.8 A/W and a maximum photocurrent of 250 mA at a wavelength of 1.55 μm.

Index Terms: p-i-n photodiodes, optical waveguides, analog optical links, optical confinement factor, waveguide photodiode

1. Introduction

Microwave photonics applications, including analog optical transmit/receive links, antenna remoting, and optical clocks, benefit tremendously from photodiodes exhibiting high responsivity, wide bandwidth, high linearity, and high power operation. Efforts to increase the photocurrent handling capabilities of photodiodes have included work on surface-illuminated photodiodes [1,2], waveguide photodiodes [3,4], and traveling-wave photodiodes [5,6]. Two dominant effects that limit the maximum photodiode output photocurrent are space-charge screening in the photodiode drift region and inadequate heat dissipation. For sufficiently high optical input powers, the electric field created by the space-charge can become so strong that the bias electric field will collapse, resulting in photocurrent compression [2].

For high-current photodiodes, linearity and thermal dissipation are limited by the area over which the optical power is absorbed. Previously, distributed-absorption waveguide structures have been studied to increase the photodiode absorption length [3]. In this paper, we report on the first demonstration of a high-current, high-responsivity waveguide photodiode based on the slab-coupled optical waveguide (SCOW) concept. This device was designed to have an ultra-

This work was sponsored by the United Stated Air Force under Air Force contract number FA8721-05-C-0002. The opinions, interpretations, conclusions and recommendations are those of the authors and are not necessarily endorsed by the United States Government.

low optical confinement factor Γ and relatively low excess loss, which allows for the extension of the absorption length beyond 2 mm.

2. Low-Confinement Waveguide Photodiodes

The optical power in a waveguide photodiode, as a function of the propagation distance z from the input facet of the waveguide, can be written as:

$$P(z) = \eta_C P_{IN} e^{-(\Gamma\alpha_o + \alpha_i)z} \tag{1}$$

where η_c is the input coupling efficiency, P_{IN} is the optical input power, α_o is the absorption coefficient of the absorbing layer ($\alpha_o \sim 6000$ cm^{-1} for bulk InGaAs at a wavelength of 1550 nm), and α_i is the excess absorption coefficient. Using Eq. (1), the detection efficiency of a waveguide photodiode is defined as the optical power that is detected and converted into photocurrent P_{DET} divided by P_{IN}. Using Eq. (1), the detection efficiency of a waveguide photodiode can be expressed as:

$$\eta_{DET} = \frac{P_{DET}}{P_{IN}} = \frac{\eta_C \Gamma \alpha_o}{\Gamma\alpha_o + \alpha_i}\left[1 - e^{-(\Gamma\alpha_o + \alpha_i)L}\right] \tag{2}$$

where L is the total length of the device. In order for waveguide photodiodes to achieve both high detection efficiency and long absorption length, two criteria must be met. First, the active absorption $\Gamma\alpha_o$ must be kept low and second, the excess optical absorption α_i must be kept to a minimum. Two cases of the simulated photodiode detection efficiency as a function of device length are shown in Fig. 1. Each case is plotted for a range of α_i from 0.1 cm^{-1} to 5.0 cm^{-1}, for a total device length up to 1 cm and for an input coupling efficiency η_c of 100%.

The excess absorption coefficient α_i in a waveguide photodiode is determined by several factors, including free-carrier absorption in the various material layers and waveguide scattering losses. The minimum α_i can be bounded by the loss present in a bulk material that would be used for the waveguide layer. For InP-based structures operating at a wavelength of 1.5 μm, the minimum α_i is ~ 0.1 cm^{-1}, as measured by Ballman [7]. We use this value as a lower limit in our analysis.

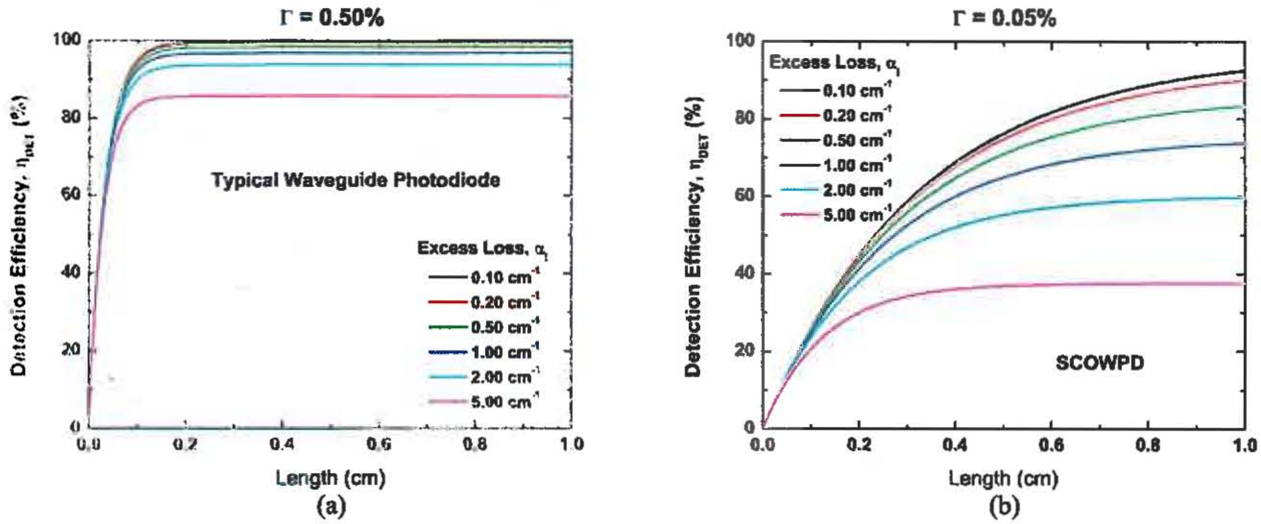

Fig. 1. Detection efficiency as a function of waveguide photodiode length for a range of excess optical loss for (a) a waveguide photodiode, having Γ = 0.50%, and (b) a waveguide photodiode, having Γ = 0.05%.

For waveguide photodiodes that have been demonstrated prior to this work, Γ is in the range of 0.50% to 20.0% [8-11]. In Fig. 1(a), we calculate the detection efficiency for the lower end of this range (Γ = 0.50%). For Γ = 0.50%, a detection efficiency greater than 85% can be achieved for $\alpha_i \leq 5.0$ cm^{-1} for a total device length less than 1 mm. This device has a low sensitivity to changes in α_i, which is a positive feature. However, it also has a short absorption length, making it susceptible to saturation and overheating at high-power operation. The second case, Fig. 1(b), shows the calculated detection efficiency for a waveguide photodiode with Γ = 0.05%, one order of magnitude smaller than the first case. The calculated detection efficiency in Fig. 1(b) shows that α_i must be kept to a minimum to achieve the same maximum efficiency as in Fig. 1(a) for a waveguide photodiode with a total length of 1 cm. As shown in the plot, this case is very sensitive to small changes in α_i and it is necessary to maintain α_i below 0.2 cm^{-1} in order to achieve a detection efficiency greater than 85% for a 1-cm-long waveguide photodiode with Γ = 0.05%. The ultra-low Γ plays a very important role in allowing the absorption of high optical powers to be distributed over a much longer length, and therefore avoid being limited by saturation or overheating. In this work, we present a long waveguide photodiode with an ultra-low Γ and an increased absorption length of 2.1 mm, designed for high-power operation. Descriptions of the device design, fabrication, and characterization are presented in the next two sections.

Previously, waveguide photodiodes with decreased Γ for increased power handling and a longer absorption length have been demonstrated [3,8,9,12]. Table 1 compares the Γ, device length, and maximum photocurrent of these devices to the device presented in this work. We present a waveguide photodiode having an ultra-low Γ ~ 0.05%, which allows for high-power operation (300 mW input optical power generating 250 mA of photocurrent) over a long absorption length (2.1 mm). The most comparable result for maximum photocurrent is from Shubin et. al., for Γ = 5.0%, whose device was capable of handling nearly 600 mW of input optical power. Due to thermal limitations in our current implementation, the waveguide photodiode presented in this work cannot handle input optical powers beyond ~ 350 mW. Thus, the maximum achievable

photo-generated current is limited, even with a high responsivity. The causes of these thermal limitations are discussed later in the paper.

Optical Confinement Factor Γ (%)	Length (μm)	Photocurrent (mA)	Reference
5.0	1200	222	[8]
1.5	200	80	[12]
0.5	300	17	[9]
0.15-1.5	300	144	[3]
0.05	10000[(1)] 2100[(2)]	250	This Work

Table 1. Waveguide photodiode with ultra-low optical confinement factor presented in this work compared to other efforts to decrease the optical confinement factor to enable high power operation. [(1)]Total waveguide photodiode length. [(2)]Waveguide photodiode absorption length.

3. SCOWPD Device Description

The SCOW concept is based on Marcatili's application of coupled mode theory, which states that a multimode waveguide can operate single mode if the multimode waveguide is appropriately coupled to a slab waveguide [13]. With the correct selection of waveguide dimensions, the lowest-order fundamental mode propagates with minimal loss, while the higher order modes radiate away into the slab with high loss. This concept enables the realization of a large, single-mode waveguide capable of handling high optical powers. By including quantum wells in the SCOW structure, both high-power lasers [14] and amplifiers [15] have previously been demonstrated. In this work, we have applied the SCOW concept to realize an InGaAsP/InP slab-coupled optical waveguide photodiode (SCOWPD) with a total length of 1 cm and a $1/e$ absorption length of 2.1 mm [16]. This SCOWPD operates at 1.55 μm and has an ultra-low $\Gamma \sim$ 0.05%.

Shown in Fig. 2 is a cross-section of the SCOWPD device, which illustrates how the fundamental waveguide mode propagates in the thick InGaAsP waveguide, having very low overlap with both the InGaAs absorption layer and the lossy p-InP cladding layer. The dimensions of the ridge width, ridge height, waveguide thickness, and slab thickness were carefully selected, using Marcatili's SCOW concept, to enable both single-mode device operation and an ultra-low optical confinement factor Γ. The SCOWPD material structure reported here was grown on a semi-insulating InP substrate via organo-metallic vapor-phase epitaxy (OMVPE). The device structure consisted of an undoped InP cladding layer (1 μm), an undoped InGaAsP waveguide layer (3 μm), an n-InGaAsP waveguide/contact layer (1 μm, Si = 5×10^{17} cm^{-3}), an undoped InGaAsP waveguide/sweep-out layer (1 μm), an undoped InGaAsP to InGaAs graded layer (35 nm), a very thin undoped InGaAs absorber layer (20 nm), a p-InP

cladding layer (1 μm, Zn = 1x10^{18} cm^{-3}), a p-InP to p-InGaAs graded layer (100 nm, Zn = 1x10^{18} cm^{-3}), and a p-InGaAs contact layer (100 nm, Zn ~ 3x10^{18} cm^{-3}). One-dimensional mode simulations show that an optical confinement factor of $\Gamma \sim 0.05\%$ can be achieved with a 20-nm-thick InGaAs absorbing layer, as shown in Fig. 3. Furthermore, BPM simulations predict an ultra-low optical confinement factor ($\Gamma = 0.066\%$) and low excess loss ($\alpha_i = 0.37$ cm^{-1}) for a 20-nm-thick- InGaAs absorber. These predicted values of Γ and α_i would result in a 1/*e* absorption length of approximately 2.31 mm.

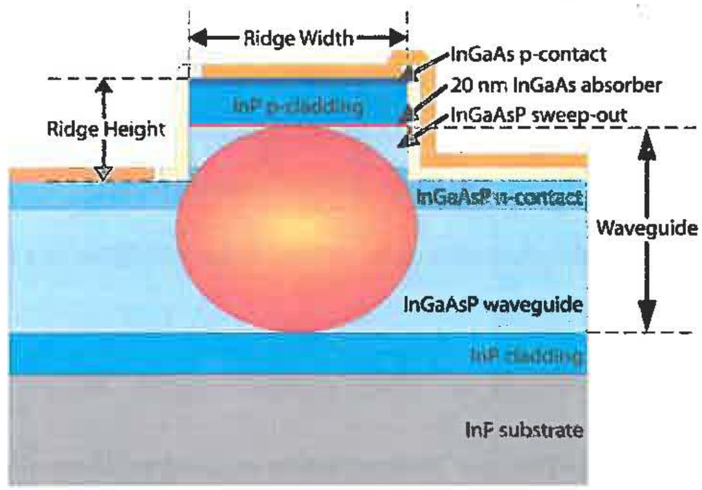

Fig. 2. Cross-section of the SCOWPD, showing the fundamental mode location and overlap with the InGaAs absorber, ridge height (2.75 μm), ridge width, and thick waveguide (5 μm).

The waveguide ridges were defined by a $Cl_2/SiCl_4/Ar$ inductively coupled plasma reactive ion etch (ICP-RIE), followed by a short wet etch. The dimensions consisted of a ridge height of h = 2.75 μm and varying ridge widths of w = 4, 5, 6, 7, or 8 μm. Following this, the samples were passivated with a 5% $(NH_4)_2S$ in DI water solution, and then immediately coated with a 2900 Å SiO_2 film to provide electrical insulation [17]. N-metal (Ge/Au/Ni/Au) and p-metal (Ti/Pt/Au) contacts were deposited and annealed [14,15]. The 1-cm-long device was divided into 20 electrically isolated sections, each 500 μm long, by wet etching the p-InGaAs cap layer and performing a proton implantation between each section. This segmented electrode allowed the photogenerated current to be measured as a function of distance from the input facet in order to determine the absorption length. Finally, the SCOWPDs were cleaved to a length of 1 cm and the front and back facets were treated with 5% $(NH_4)_2S$ in DI water before the anti-reflection coating was applied. The devices were mounted junction-side up with indium solder to Ti/Pt/Au sputtered copper submounts.

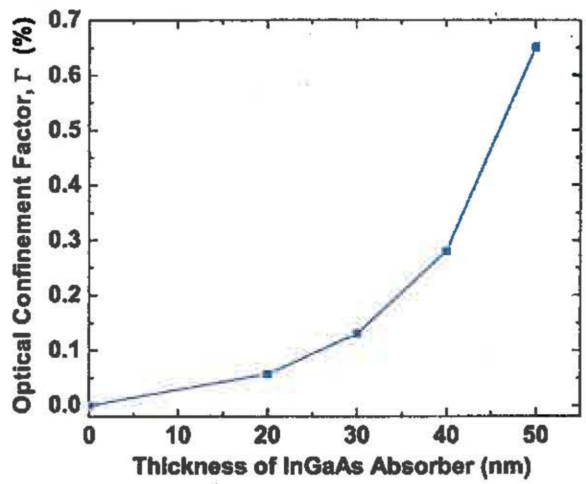

Fig. 3. One-dimensional (1-D) mode calculations of the optical confinement factor as a function of InGaAs absorber thickness.

4. Results and Discussion

Dividing the 1-cm-long SCOWPD into 20 electrically isolated sections allowed for the photo-generated current to be measured as a function of distance from the input facet. This was achieved using on-wafer probing with a 20-contact DC probe head. Top-view photographs of the multi-section SCOWPD chip are shown in Fig. 4, with increasing detail and magnification from top to bottom. The top photo shows a full bar for bench top testing, containing ten complete 20-section devices. The middle photo shows a section of that bar, illustrating how the devices are positioned. The bottom photo shows the most detail, indicating the location of the n- and p-contacts, the waveguide, and the implant isolation. The measurement configuration was automated to control a source-measure unit, for biasing the SCOWPD and measuring dark current and photocurrent, and a 20-channel relay switch, for applying the appropriate bias to each section. Two voltage supplies were used in the measurement configuration. The first was used to appropriately bias the section under test and the second was used to hold the remaining 19 sections at a constant bias. Figure 5 is a schematic of the measurement configuration, depicting the 20-contact DC probe head as a switch. The optical components of the experimental set-up included a tunable laser, an erbium doped fiber amplifier (EDFA), a variable optical attenuator, a polarization controller, and a lensed fiber.

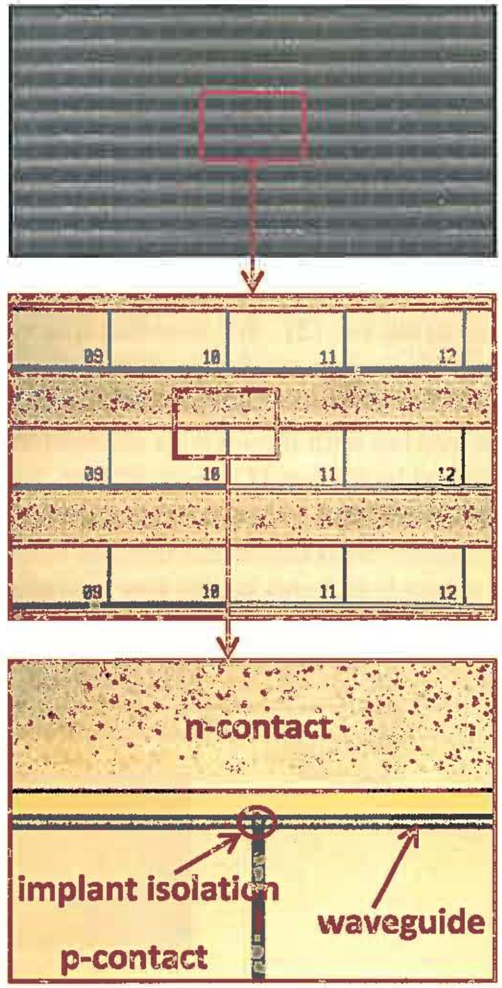

Fig. 4. Top-view photographs of the multi-section SCOWPD chip, shown with increasing magnification from top to bottom.

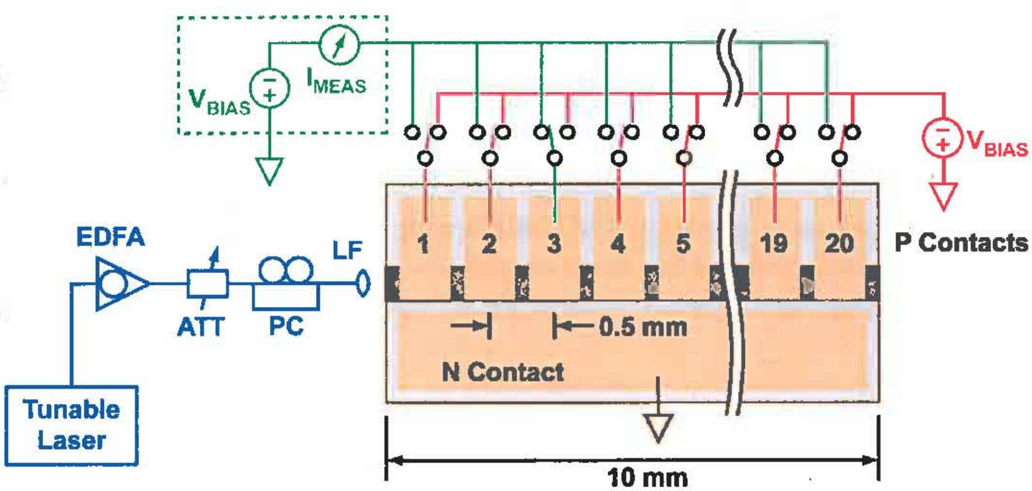

Fig. 5. SCOWPD measurement configuration, showing section 3 connected to a source-meter and the remaining sections connected to a fixed voltage source.

Figure 6 shows the distribution of photocurrent along the length of a 1-cm-long SCOWPD having $w = 6$ µm. These data were obtained by fiber coupling a 1550-nm CW laser signal to the AR-coated input facet using a lensed fiber with a 6.5-µm spot size. The photodiode was reverse biased to −3 V. For an optical input power of 20 mW, the total photocurrent for this device, with all 20 sections biased, was 16.4 mA, corresponding to an external responsivity of $R = 0.82$ A/W. Excluding the first data point, the photocurrent decay as a function of device length can be fit to a simple exponential. From this fit, the total absorption coefficient was determined to be $\Gamma\alpha_o+\alpha_i = 4.8\ \text{cm}^{-1}$. Using this value of $\Gamma\alpha_o+\alpha_i$, and assuming zero background loss ($\alpha_i = 0$), an upper bound of $\Gamma = 0.08\%$ is calculated using Eq. (2). We note that this value of Γ is nearly half the smallest value reported elsewhere [3], and in good agreement with the desired ultra-low Γ. The likely explanation for the increased photocurrent in the first section is that the launched beam profile has a larger Γ (i.e., more overlap with the InGaAs absorption layer) than the fundamental waveguide mode. The mis-launched beam would then evolve to the waveguide mode over some propagation distance in the first section, and Γ would decrease to the as-designed ultra-low Γ. It is unlikely that the increased photocurrent is due to the thermal effects described below since the total current in the first section is less than 6 mA in this low power measurement.

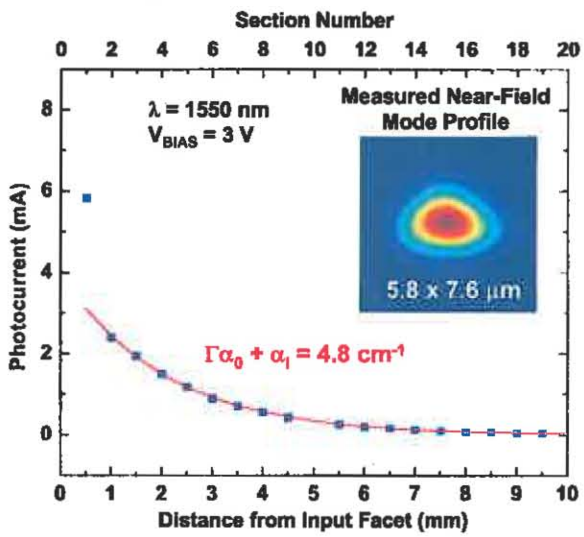

Fig. 6. Photocurrent as a function of distance from the input facet of the SCOWPD. Inset shows the near-field mode profile.

The measured near-field mode profile of a SCOWPD with $w = 6$ µm is shown as an inset to Fig. 6. The $1/e^2$ intensity dimensions of this mode are 5.8 µm x 7.6 µm. Mode-overlap calculations predict a 92% input coupling efficiency between the 6.5-µm-spot-size lensed-fiber mode and the SCOWPD mode.

To obtain a better estimate of the optical confinement factor and excess optical loss of the SCOWPD structure, we used the data of Fig. 6 to compute the maximum detection efficiency, assuming 100% coupling efficiency. Figure 7 shows the measured detection efficiency as black squares for a SCOWPD with $w = 6$ µm. Fitting Eq. (2) to the data (red curve) allowed us to extract estimated values for Γ and α_i, assuming ideal coupling conditions. Due to the outlying data point from the first section of the device, the extracted values are only estimates. The

optical confinement factor estimated from measurements ($\Gamma = 0.069\%$) shows excellent agreement with the ultra-low optical confinement factor predicted by BPM simulations ($\Gamma = 0.066\%$). However, the excess loss estimated from measurements ($\alpha_i = 1.65\ \mathrm{cm}^{-1}$) is significantly higher than the predicted value ($\alpha_i = 0.37\ \mathrm{cm}^{-1}$). This larger than expected excess optical loss results from non-ideal coupling, excess waveguide scattering, Zn diffusion from the p-doped InP, larger than expected loss from the n-doped region which has high overlap with the mode, or a combination of the above. If a coupling efficiency of 80% is assumed instead of 100%, for example, the estimated α_i drops to ~ $1.0\ \mathrm{cm}^{-1}$. In Fig. 7, the green and blue regions correspond to the effect that changes in Γ and α_i have on detection efficiency for a coupling efficiency of 100%. The upper bound of the green region and the lower bound of the blue region are representative of $\Gamma = 0.15\%$, $\alpha_i = 0.10\ \mathrm{cm}^{-1}$ and $\Gamma = 0.03\%$, $\alpha_i = 2.0\ \mathrm{cm}^{-1}$, respectively.

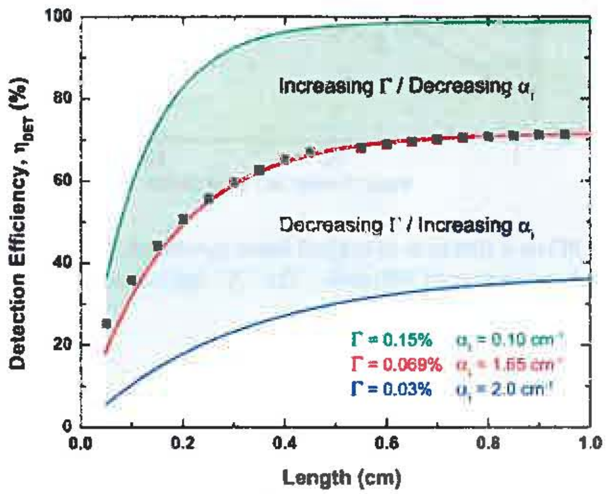

Fig. 7. Detection efficiency as a function of device length for a SCOWPD with $w = 6\ \mu\mathrm{m}$. Measured data results in $\Gamma = 0.069\%$ and $\alpha_i = 1.65\ \mathrm{cm}^{-1}$. As Γ increases and/or α_i decreases, the detection efficiency improves.

As mentioned earlier, one of the main goals of implementing the SCOWPD device structure was to increase the maximum photocurrent that can be generated. Figure 8 shows a log-log plot of the zero-impedance-load photocurrent as a function of optical input power at the facet for a SCOWPD with a $w = 5\ \mu\mathrm{m}$ ridge. For an optical input power of 300 mW, the total photocurrent generated in the 1-cm-long SCOWPD was 250 mA. To our knowledge, this is the highest photo-generated current demonstrated for a waveguide photodiode device. The external responsivity R of this device remained constant at 0.5 A/W for optical input powers from 1 mW to 50 mW. Above 50 mW, R began to increase with increasing optical input power, reaching a value of 0.83 A/W at 300-mW input power. We attribute this nonlinear responsivity to thermally induced increases in some combination of Γ and α_o. First, Γ will increase in a SCOW structure if the refractive index of the p-InP cladding layer increases due to heating of this layer [18]. Second, α_o will increase with heating of the InGaAs absorber layer because the InGaAs bandedge shifts to longer wavelengths with increased temperature. Heating of the p-InP cladding and InGaAs absorber layers can be caused by both a high series resistance of the p-InP layer, caused by insufficient doping, and a high contact resistance of the metal-semiconductor interface. Optimization of the current implementation of the SCOWPD includes reducing both the electrical heating and the thermal impedance. Efforts to reduce the electrical heating of the device include an improved p-contact metallization and alloy and a higher p-InGaAs doping

level. The thermal impedance of the device will be reduced through improved mounting techniques, including optimization of the backside base metallization for soldering and the solder reflow procedure.

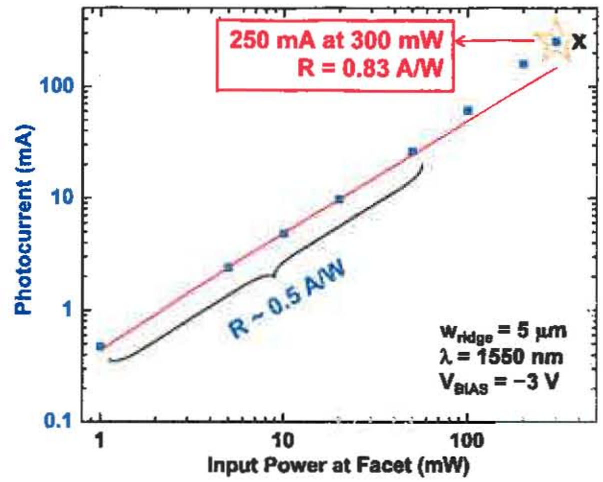

Fig. 8. Photocurrent of a SCOWPD as a function of optical input power. A record waveguide photocurrent of 250 mA was generated for an optical input power of 300 mW. The "X" indicates the optical power where the device failed.

5. Conclusion

Fundamental limitations to the maximum absorption length of waveguide photodiodes have been investigated. Specifically, we have analyzed how an ultra-low optical confinement factor Γ and an excess optical loss α_i that approaches the lower limit of ~ 0.1 cm^{-1} affect the absorption length and the detection efficiency of a waveguide photodiode. We have implemented a waveguide photodiode design, based on the SCOW concept, which begins to approach these limits. This SCOWPD device has a fundamental optical mode that has low overlap with both the absorption region and the lossy p-doped cladding layer. This has allowed for an ultra-low optical confinement factor Γ of 0.069% and a 1/*e* absorption length of 2.1 mm. Assuming 100% coupling efficiency, the excess optical loss was estimated to be 1.65 cm^{-1}. This value is larger than expected, resulting from non-ideal coupling, excess waveguide scattering, Zn diffusion from the p-doped InP, n-doped region absorption, or a combination of the above. The SCOWPD has demonstrated an external responsivity of up to 0.83 A/W and has produced a record photocurrent for a waveguide photodetector of 250 mA at 1.55 μm. By lowering the p-contact resistance with material and metallization improvements and removing the photo-generated heat with better mounting techniques, we expect that Ampere-class SCOWPD devices should be possible.

References

[1] D. A. Tulchinsky, X. Li, N. Li, S. Demiguel, J. C. Campbell, and K. J. Williams, "High-saturation current wide-bandwidth photodetectors," *IEEE J. Select. Topics Quantum Electron.*, vol. 10, no. 4, pp. 702-708, 2004.

[2] K. J. Williams and R. D. Esman, "Design considerations for high-current photodetectors," *J. Lightw. Technol.*, vol 17, no. 8, pp. 1443-1454, 1999.
[3] S. Jasmin, N. Vodjdani, J.-C. Renaud, and A. Enard, "Diluted- and distributed-absorption microwave waveguide photodiodes for high efficiency and high power," *IEEE Trans. Microwave Theory Tech.*, vol. 45, no. 8, pp. 1337-1341, 1997.
[4] J. Harari, F. Journet, O. Rabii, G. Jin, J. P. Vilcot, and D. Decoster, "Modeling of waveguide PIN photodetectors under very high optical power," *IEEE Trans. Microwave Theory Tech.*, vol. 43, no. 9, pp. 2304-2310, 1995.
[5] V. M. Hietala, G. A. Vawter, T. M. Brennan, and B. E. Hammons, "Traveling-wave photodetectors for high-power, large-bandwidth applications," *IEEE Trans. Microwave Theory Tech.*, vol. 43, no. 9, pp. 2291-2298, 1995.
[6] K. S. Giboney, M. J. W. Rodwell, and J. E. Bowers, "Traveling-wave photodetector design and measurements," *IEEE J. Select. Topics Quantum Electron.*, vol. 2, no. 3, pp. 622-629, 1996.
[7] A. A. Ballman, A. M. Glass, R. E. Nahory, and H. Brown, "Double doped low etch pit density InP with reduced optical absorption," *J. Cryst. Growth*, vol. 62, pp. 198-202, 1983.
[8] I. Shubin, X. Xie, W. S. C. Chang, and P. Yu, "High power electroabsorption waveguide device," in *IEEE Lasers and Electro-Optics Society (LEOS) Conference*, paper TuU4, 2006.
[9] J.-S. Choe, Y.-H. Kwon, and K. Kim, "Characteristics of waveguide photodetectors at high-power optical input," *IEEE Photon. Technol. Lett.*, vol. 17, no. 4, pp. 881-883, 2005.
[10] H. Jiang, D. S. Shin, G. L. Li, J. T. Zhu, T. A. Vang, and P. K. L. Yu, "Analysis of IP3 of photodiode using equivalent circuit," *Proc. International Topical Meeting on Microwave Photonics*, pp. 83-85, 1999.
[11] H. Jiang, D. S. Shin, T. S. Liao, P. Mages, A. R. Clawson, P. K. L. Yu, "Waveguide photodiodes for high speed detection," *Proc. SPIE*, vol. 4111, pp. 259-266, 2000.
[12] J. Klamkin, A. Ramaswamy, N. Nunoya, L. A. Johansson, J. E. Bowers, S. P. DenBaars, and L. A. Coldren, "Uni-traveling-carrier waveguide photodiodes with >40 dBm OIP3 for up to 80 mA of photocurrent," *Device Research Conference (DRC),* Late news paper, 2008.
[13] E. A. J. Marcatili, "Slab-coupled waveguides," *The Bell System Technical Journal*, vol. 53, pp. 645-674, 1974.
[14] J. N. Walpole, J. P. Donnelly, P. J. Taylor, L. J. Missaggia, C. T. Harris, R. J. Bailey, A. Napoleone, S. H. Goves, S. R. Chinn, R. Huang, and J. Plant, "Slab-coupled 1.3-μm semiconductor laser with single-spatial large-diameter mode," *IEEE Photon. Technol. Lett.*, vol. 14, no. 6, pp. 756-758, 2002.
[15] P. W. Juodawlkis, J. J. Plant, R. K. Huang, L. J. Missaggia, and J. P. Donnelly, "High-power 1.5-μm InGaAsP-InP slab-coupled optical waveguide amplifier," *IEEE Photon. Technol. Lett.*, vol. 17, no. 2, pp. 279-281, 2005.
[16] S. M. Madison, J. J. Plant, D. C. Oakley, D. C. Chapman, A. Napoleone, and P. W. Juodawlkis, "Slab-coupled optical waveguide photodiode," in *Proc. Conference on Lasers and Electro-Optics (CLEO),* paper CWF4, 2008.
[17] R. S. Besser and C. R. Helms, "Comparison of surface properties of sodium sulfide and ammonium sulfide passivation of GaAs," *J. Appl. Phys.*, vol. 65, no. 11, pp. 4306-4310, 1989.
[18] P. K. L. Chan, K. P. Pipe, J. J. Plant, R. B. Swint, and P. W. Juodawlkis, "Temperature mapping and thermal lensing in large-mode, high-power laser diodes," *Appl. Phys. Lett.*, vol. 89, pp. 201110-1-3, 2006.